INTERNATIONAL ATOMIC ENERGY AGENCY
UNITED NATIONS EDUCATIONAL, SCIENTIFIC AND CULTURAL ORGANIZATION
INTERNATIONAL CENTRE FOR THEORETICAL PHYSICS
I.C.T.P., P.O. BOX 586, 34100 TRIESTE, ITALY, CABLE: CENTRATOM TRIESTE

H4-SMR 393/61

SPRING COLLEGE ON PLASMA PHYSICS

15 May - 9 June 1989

TEARING MODES IN TOKAMAK PLASMA

Lecture 1 & 2

Huo Yu Ping

Institute of Plasma Physics
Academia Sinica
Anhui, Hefei
P. R. China

Lecture one: Tearing Modes in Tokamak Plasma

1. Ideal MHD Instabilities:

(1) During the early 1950's, the main problem in Fusion Research was stablizing the ideal MHD instabilities (Sausage-like m=o and kink-like m=1 or 2 modes) which firstly were observed in Dynamic Pinch. At that time, the MHD time scale of the current devices was $\tau_h = a_h (4\pi\rho)^{1/2}/B \sim 10^{-7} - 10^{-6}$ sec.

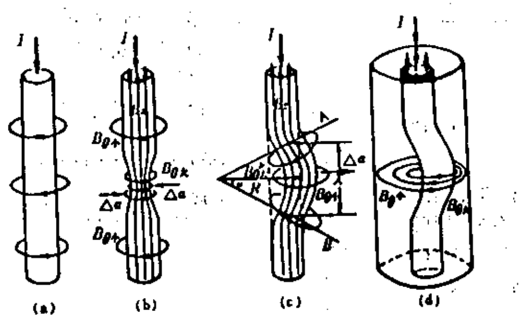

Fig. 1

Such instabilities could be stablized by strong longitudinal magnetic field and coducting wall, as shown in Fig.2. This configuration finally led to the Tokamak concept. But it was found that, the resistive interdifusion of the equilibrium field led to the onset of terminal kink instability after a timt interval about $\tau_R/10 \sim 10^{-5}$ sec.

In 1958, it was found that the stabilization of a realistic, finite edge region would call for a moderate reversal of the B_Z. It was verified by hard-core pinch experiment in Livermore, and became known in later years as RFP. But at that time it was found that, vigoorous MHD instabilites persisted even in the supposedly stable case.

(2)

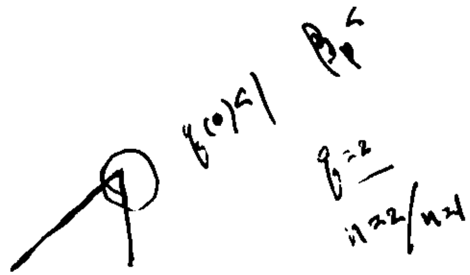

2. Tearing Mode Theory:

For PLT size Tokamak, there are two time scales:

Resistive time $\tau_R = 4\pi a^2/\eta c^2 \sim 1 - 10$ sec.

MHD time $\tau_H = (4\pi\rho)^{1/2} a/B \sim 10^{-8} - 10^{-6}$ sec.

But the growth time of tearing mode:

$$\gamma^{-1} \sim K \tau_h^{2/5} \tau_R^{3/5} \quad , \quad K = 2/((ka)^{2/5}(\Delta' a)^{4/5})$$

so the diffusion should be limited in a thin layer!

(1). Current layer model:

The linearized Ohm's law,

$$\frac{\partial \psi}{\partial t} + V_x B_{y0} = \frac{\eta c^2}{4\pi} \nabla^2 \psi$$

and equation of motion,

$$\frac{\rho}{k^2} \frac{\partial}{\partial t} \nabla_\perp V_x = \frac{B_{y0}}{4\pi} \nabla_\perp^2 \psi - \frac{\psi}{c} \frac{dj_{z0}}{dx}$$

could be solved by boundary layer method as follows:

Round the singular surface x=0, there is a thin layer.

Outer region: Ideal MHD process and so $\frac{\partial}{\partial t} \sim 0$,

$$\nabla_\perp^2 \psi - \frac{4\pi}{c B_{y0}(x)} \frac{dj_{z0}}{dx} \psi = 0$$

we have $\psi(x = \pm a) = 0$,

with . At x=0, $\psi(x)$ should be continuous, but $\frac{d\psi}{dx}$ has discontinuity: $\Delta' = \frac{-1}{\psi(0)} \left[\frac{d\psi}{dx}\right]_{x=0}$.

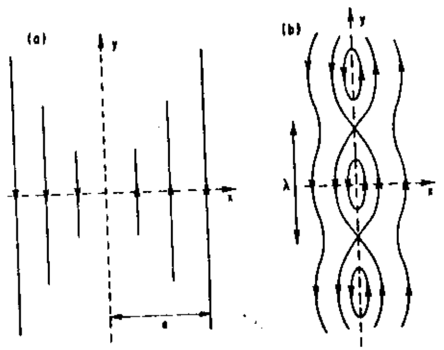

$B_y(x)$

Fig. 2

Δ' depends on the current profile $j_{z0}(x)$, but on nothing else.

Inner region: $B_{y0} = B'_{y0} x$, $\nabla_\perp^2 \psi$ much larger than $\psi dj_{z0}/dx$,

therfore $\frac{\gamma\rho}{k^2} \frac{\partial^2 V_x}{\partial x^2} + \frac{B'_{y0} x}{\eta c^2} (-\gamma\psi - B'_{y0} x V_x) = 0$.

Approximately $\psi(x) = \psi(0)$=const., and v_x is odd in x,

we easily got the width of the layer: $\delta \sim (\gamma\rho\eta c^2/k^2 B'^2_{y0})^{1/4}$,

and $\left[\frac{d\psi}{dx}\right]_{x=0} = -\frac{4\pi}{\eta c^2} \int_{-\infty}^{\infty} (\gamma\psi(x) + B'_{y0} x V_x) dx = \Delta(\gamma)$.

Finally, $\Delta(\gamma) = \Delta'$ and we got the growth rate: $\gamma^{-1} \sim \tau_H^{2/5} \tau_R^{3/5}$

$$\gamma \sim 0.5 \left(\frac{ka}{\tau_H}\right)^{2/5} \left(\frac{\Delta' a}{\tau_R}\right)^{3/5}$$

Therefore if $\Delta' > 0$, $\gamma > 0$ and the mode is unstable; if $\Delta' < 0$, $\gamma < 0$, the mode is stable. <u>The stability totally depends on the ideal MHD process in outer region!</u>

(2) Tearing mode in sylindrical case.

Resonat surfaces: $m = nq(r_s)$, $q = rB_z/RB_\theta$.

Take $B_r = im\psi/r$, $\vec{k} \cdot \vec{B} = (m - nq(r))B_\theta/r$, $J_r = m\psi/r\vec{k} \cdot \vec{B}$.

Outer region: $\nabla_\perp^2 \psi - \frac{4\pi m}{c r k \cdot B_0} \frac{dj_{z0}}{dr} \psi = 0$.

$$\delta W_p = -\frac{1}{2} r_s \Delta' \psi(r_s)^2 \quad , \quad \Delta' = \frac{1}{\psi(r_s)} \left(\frac{d\psi}{dr}\right)_{r_s}$$

For ideal MHD kink mode, J_r must be finite everywhere within the plasma, if $r_s < a$, $\psi(r_s) = 0$, therefore $\delta W_p = 0$.

The only possibility is that r_s falls in vacum region. But in resistive case $\psi(r_s)$ can be nonzero.

Solve Eqn.(1) numerically for three current profile cases:

$$j_z(x) = j_z(0)/(1 + x^{2p})^{1+1/p} \qquad p = 1,2,3$$

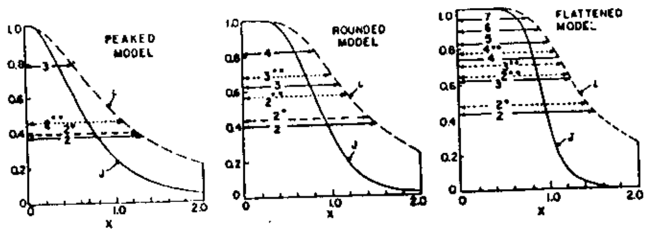

Fig. 3 Three representative tokamak current profiles and their tearing-mode stability properties. A mode with a given m-value (2,3,4,etc.) is unstable if its singular surface falls within the region indicated by the arrows. In the case $2^*, 3^*$, etc., there is a conducting wall at $x_b = 2$, in the cases $2^{**}, 3^{**}$, etc., the wall is at $x_b = 1.33$; otherwise there is no conducting wall.

A mode of m is unstable if its singular surface falls within in the range of x indicated by the arrows.

$\sim \varepsilon \approx \frac{a}{R}$

(3) Toroidal geometry:

Simple case: Mode has three m components, m-1,m,m+1;

only r_m and r_{m+1} are inside the plasma.

Between resonat surfaces, ideal MHD process

marginal equation:

$$L_{m-1}\psi_{m-1} = K_{m-1}^{m}\psi_m + K_{m-1}^{m+1}\psi_{m+1}$$
$$L_m\psi_m = K_m^{m-1}\psi_{m-1} + K_m^{m+1}\psi_{m+1}$$
$$L_{m+1}\psi_{m+1} = K_{m+1}^{m-1}\psi_{m-1} + K_{m+1}^{m}\psi_m$$

The soluble condition for the boundary conditions:

$$\psi(a)=0,\quad \psi_m'(r_m)/\psi_m(r_m)=\Delta_m',\quad \psi_{m+1}'(r_{m+1})/\psi_{m+1}(r_{m+1})=\Delta_{m+1}',$$

is $\quad (\Delta_m' - \alpha)(\Delta_{m+1}' - \beta) = \gamma$

From the solutions in inner layers(r_m and r_{m+1}), we have

$$\Delta_m' = \Delta_m(\omega) \quad , \quad \Delta_{m+1}' = \Delta_{m+1}(\omega) .$$

Therefore the dispersion relation is:

$$(\ \Delta_m(\omega) - \alpha\ )\ (\ \Delta_{m+1}(\omega) - \beta\ ) = \gamma$$

Real example: m=1, m+1=2, m-1=0 resonant surface is out of (0,a) region. The finite solution shows that, the coupling (m+1 component of m mode) is always proportional to ε = a/R.

$\varepsilon \sim \frac{a}{R}$

(4) Non-linear development of the tearing mode. The non-linear tearing mode theory mainly deals with the behavior of finite size.

The non-linear Ohm's law is:

$$\frac{\partial}{\partial t}\psi + \vec{v}\cdot\vec{\nabla}\psi = \frac{\eta c^2}{4\pi}\nabla^2\psi$$

For imcompressible low β plasma: $\quad \vec{v} = \vec{z}\times\vec{\nabla}\phi$,

$$\rho\left(\frac{\partial}{\partial t} + \vec{v}\cdot\vec{\nabla}\right)\nabla^2\phi = -\frac{\vec{z}}{c}\cdot(\vec{\nabla}\psi\times\vec{\nabla}j)\ ,\quad j=-\nabla^2\psi$$

Define: $\quad W = 4(\psi/\psi'')^{1/2}$

For small W(W< δ), $\quad \frac{\partial}{\partial t}\psi \approx \gamma\psi''$,

$$\psi'' \sim \frac{\psi_+' - \psi_-'}{\delta} \sim \frac{\Delta'}{\delta}\psi$$

<u>i.e. W increases linearly with time.</u>

For W> δ, $\quad \psi'' \sim \frac{\Delta'\psi}{W} \implies \frac{\partial}{\partial t}W = \frac{1}{2}\eta\Delta'(W)$.

More detail analysis shows that:

$$\frac{\partial}{\partial t}W = \frac{1}{2}\eta\Delta' + j_0\frac{d\eta}{d\psi}W$$

<u>Finally W will saturate when</u> $\quad \Delta'(W) = 0$,

or $\quad \Delta'(W) = 2\frac{j_0}{\eta}\left(-\frac{d\eta}{d\psi}\right)W$

Generally, Peak j(r) profile -> small island;

flat-topped , square-shaped j(r) -> large W.

Fig.4 shows the formation process of disruption.

Slow-growing 2/1 mode (fast linear growth is hardly seen);

m=2 island flatens q(r) around q=2, and steepens q(r) at 3/2;

3/2 mode appears and flatens q(r) around q=3/2;

5/3 mode grows in turn and so forth;

Some magnetic surfaces be ergodic and a catastrophic disruption occurs.

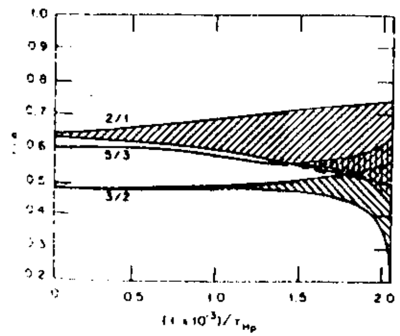

FIG. 4 Computer simulation of tokamak resistive kink modes[14] shows the growth of the n = 1, m = 2 mode destabilizing first n = 2, m = 3 and then n = 3, m = 5 mode

(5) Helical winding experiments and modes coupling.

* Experimental results of Pulsator and other devices:

Suppressing 2/1 fluctuation;

Delay the major disruption;

Existing a threshord for disruption;

Stopping the rotaion of the Mirnov's signal.

* Theoretic calculation from simple tearing mode theory.

The RHF is very weak, can only influence the magnetic structure near q=2 surface, and then suppress 2/1 mode.

* In l=2/n=1 helical coordinate system

RHF-->magnetic island

-->flaten j(r) round q(r)=2

Initial value numerical method

--> growth of perturbation

RHF delay the development of the mode only but do not change the saturation level.

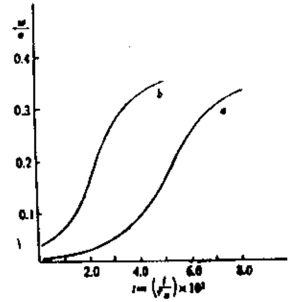

图 5

a 为加螺旋场; b 为不加螺旋场

* RHF suppress the mirnov's signal can not be totally due to stopping the toroidal rotation.

NB injection : rotation increases fast, but frequency change a little.

Why it can suppresses the disruption.

* HT-6B Experients:

Device: R=45cm, a=12.5cm, B_t=0.7-1.0 T, I_p=50kA.

L=2/n=1 and l=3/n=1 helical winding, sidebands are smaller than 15% of the corresponding main components.

I_h < 1% I_p.

m=2,3,4,5 cos coils, soft x ray detector array, ECE measurment, visible and VUV multi-chennel spectroscopy, Langmuir probs and some conventional diagonostics.

l=2 RHF results. A1

l=3 RHF results. A2

Effect of the combination of l=2 and l=3 RHF. A3

Amplification of sawtooth oscillation. Λ4

All the forementioned phenomena have been checked on HT-6M and Text Tokamaks.

* Global mode structure:

RHF are very weak, less than 1% of the poloidal field, they only can influence directly the magnetic configuration near the corresponding resonant surfaces(localized resonsnt disturpances).

l=2 RHF can suppress all m=2, 3, 4, 5 magnetic fluctuations which have the same frequency. One possible explanation is, all m=3, 4, 5 signals are the sideband components of m=2 mode.

But l=3 RHF also can suppress all m=2, 3, 4, 5 fluctuations and perhaps, more effectively. It means that, in the structure of observed mode the m=3 component and q=3 surface have the same position as m=2 component and q=2 surface.

l=3 RHF can mantain the dicharge even after turning on a l=2 RHF which is higher than the disruption threshord.

Therefore, we really observed a global mode which has different components mainly located around different q surfaces.

* Preliminary theoretical consideration.

If we insist in the tearing mode scope, we should go back to to the resistive MHD equations in toroidal geometry, and consider the coupling terms of different m components as singular perturbation near resonant surfaces.

It could be proved that, the toroidal term can only introduce the coupling proportional to $\varepsilon=a/R$. But it seems hopeful that, the non-linear coupling terms can mix different m components and form some modes with global structure.

Lecture Two: Sawtooth Oscillation in Tokamak

1. MHD instability and transport process

MHD motion of the plasma are tightly connected with trasport process.

(1) Profile consistancy:

* Due to the fact that the magnetic island enhances local trasport, one of the possible results of growth of different tearing modes is to

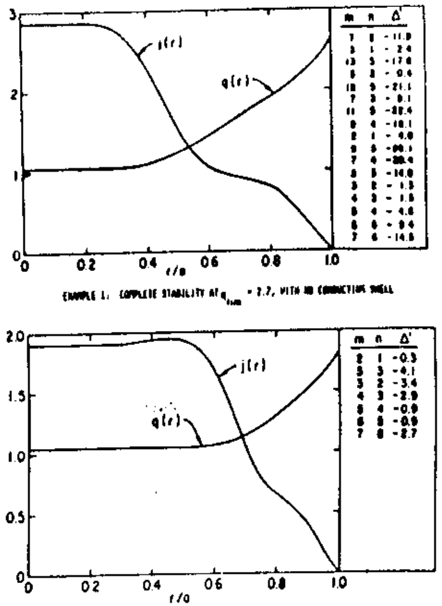

Fig. 5

realize a j(r) profile stablizing all the tearing modes, as Fig. 5.

* It has been found that, on some devices, the relative electron temperature($T_e(r)/T_e(0)$) has the same profile for different discharge parameters and different heating power.

  low q_L discharge: trapezoidal shape. Fig. A5

  high q_L discharge: strong central peaking. Fig. A6

(2) Sawtooth oscillation and the influences of the helical field. A7

2 Basic phenomena and classical model:

* Since 1974, the first observation on ST, sawteeth oscillation has been one of the most important processes in Tokamak plasma and has been studied widely.

  Central part heating

  -> j(0) increases

  -> q(0) decreases

  -> collapse

  -> central flatening

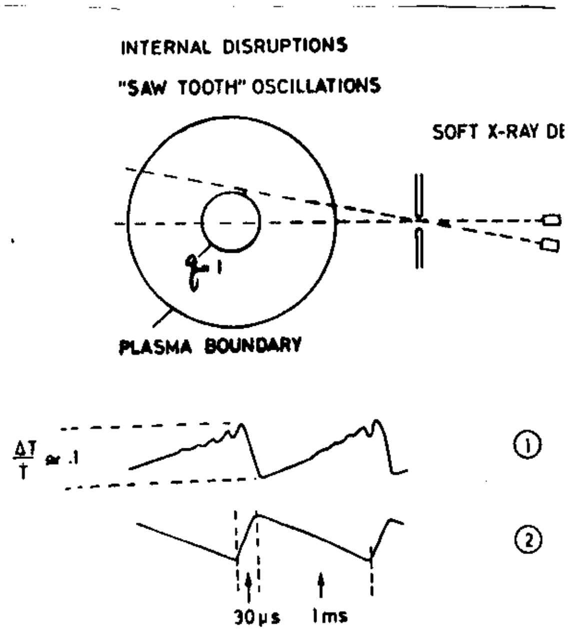

Fig. 7 Experimental set-up for observation of sawtooth oscill

Outside q=1 surface temperature suddenly increase due to the the central collapse, then decaying by diffusion.

The collapse is m=0 symetric, just before it there is m=1 precursor.

Soft x ray signal of sawtooth is mainly due to the temperature oscillation(TFR's results)

(1) 1970 Shafranov analized m=1 ideal MHD mode, which is unstable for q<1 as p'< 0.

1973 Rosenbluth, et al. analized the non-linear behavior of ideal m=1 mode, the saturated displacement turned out to be too small compared with experimental values.

(2) 1975 Kadomtsev proposed that, collapse is due to the rapid reconnection of the helical flux inside q=1 surface to that of outside. The resistive diffusion only take place in a narrow layer at the q=1 surface, Fig. 8.

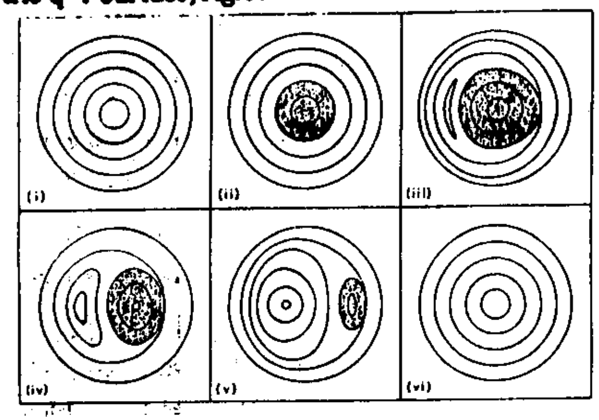

Fig. 8 Development of magnetic field structure during the sawtooth collapse according to Kadomtsev model. The m=1 instability displaces the q < 1 region (shown shaded) and restores q to a

(3) 1975 Sykes et al. discovered from numerical calculation, and Bussac et al. from analytical investigation that, m=1 ideal MHD mode is stable below a critical value by toroidal coupling.

1976 Coppi et al. found that, resistive m=1 mode should be unstable if there is q=1 surface in the plasma. It could combine with Katomtsev's reconnection model to provide an explenation of the sawtooth collapse.

3 Sawtooth amplified by helical field

(1) Experimental results:

- L=2 RHF could amplify the sawtooth oscillation but change the period a little. This RHF also could suppress m=1 fluctuation of soft x ray signals.
- L=3 RHF plays the same roll as L=2 RHF but more effectively. In such case q=3 surface is very near the plasma edge.
- These phenomena seem to tightly connect with suppressing m=2, 3, 4 MHD modes by RHF, and depend on the impurity level.
- In some cases, sawtooth could not be observed, only m=1 fluctuation existed in soft x ray signals. Turning on the RHF could make the sawtooth oscillation appear.

(2) Comparing with amplifying sawtooth by additional heating, the conclusion seems can be got that, RHF can improve the energy confinement of the central core of the plasma, no matter which q surface the RHF can directly influence.

Sawtooth oscillation seems tightly connect with tearing mode even in heating phase.

4 Recent experimental results which can not be explaned by Katomtsev's reconnection process.

(1) On JET and, in some cases, on TFTR, the sawtooth collapse was presursorless and very rapid. The collapse time was near 100 μs, which is ten times smaller than the value predicted by Katomtsev's model.

But on TFTR the sawtooth collapses of 1 ms also have been observed.

(2) The analysis of TFR experiments indicated that, although an magnetic island was formed its growth was limited and it did not undergo a complete reconnection.

The compound sawtooth also has been observed on JET and TFTR, which shows that the magnetic island could not undergo a complete reconnection in single sawtooth collapse.

(3) On TEXTOR Tokamak, the measurement by the Faraday rotation of a lasser beam passing through the plasma gave the q(0) value much less than 1.(0.6-0.7). But on Asdex, the measurements using the Zeeman splitting of a lithium beam gave $q(0) \approx 1.05 \pm 0.05$.

No existing collapse picture can explane these results.

(4) Monster Sawtooth:

The Monster sawtooth has been observed on JET and also on TFTR by high power heating. Fig. 9

It might be regarded as an transient stabilisation of the sawtooth instability.

(5) Sawtooth amplified by RHF.

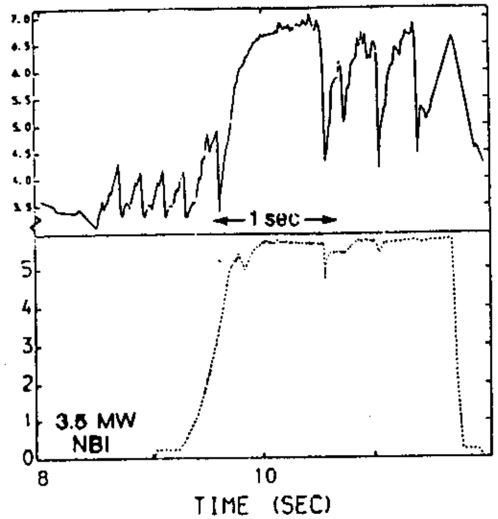

Fig. 9

(5) the new possibilities to stablize the sawtooth instability

(1) By LHCD, confirmed on ASDEX.

Broadens the current profile and raises the q value above unity everwhere.

(2) By sufficient additional heating, on JET and TFTR.

The sawtooth collapse was delayed for more than a second (3-5 energy confinement times).

The long wavelength coherent MHD activity also was very low.

The energy confinement time can be 15%-20% higher than in the normal sawtoothing regime. Fig. 10

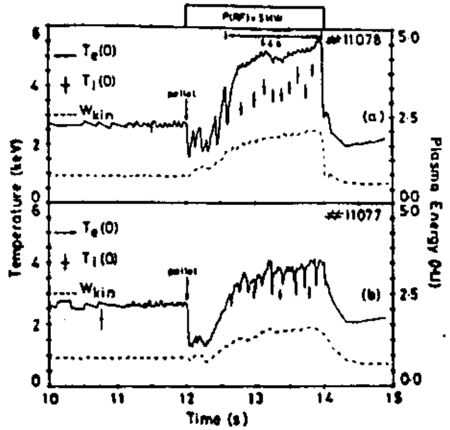

Fig. 10

A1

3. L=2/n=1 RHF of suitable value not only can suppress **m=2/n=1** fluctuation, but also can suppress **all other m** (3/1,4/1 and 5/1) modes. The near **20kHz peak** in FFT of magnetic signals disappeared totally after the L=2 RHF turning on. Obviousely, ***the m=3, 4 or 5 modes are tightly coupled with q=2 surface !***

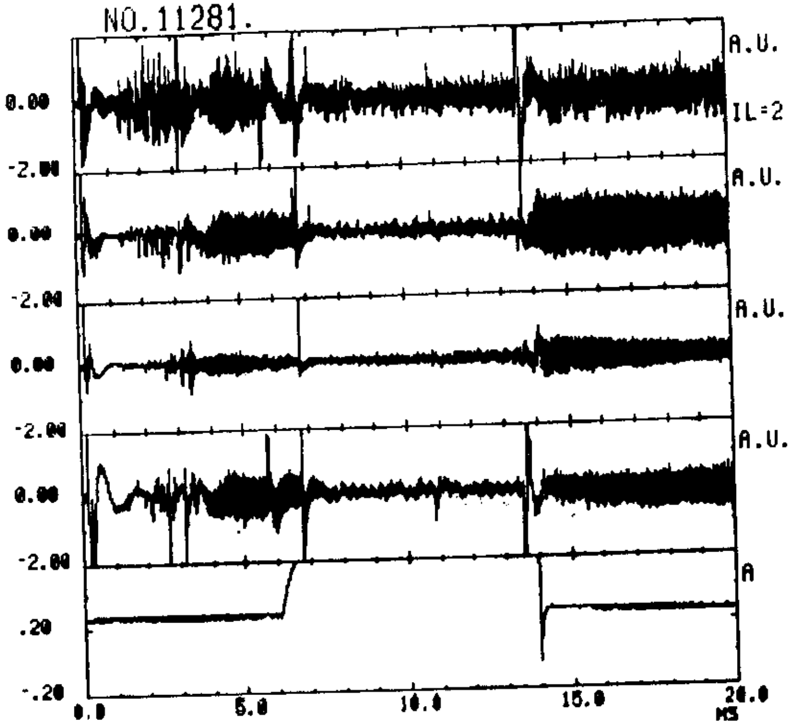

FIG.5A. GLOBLE MODE EFFECT OF RHF L=2

A2

4. L=3/n=1 **RHF** can directly only couple with q=3 surface. But not only m=3/n=1 but also m=2/n=1, m=4/n=1 modes all are suppressed by L=3 RHF, perhaps more effectively than by L=2 field.

Such phenomena also have been observed on HT-6M . It means that, the coupling between different m modes **do not** be weakened as minor radiu a increases.

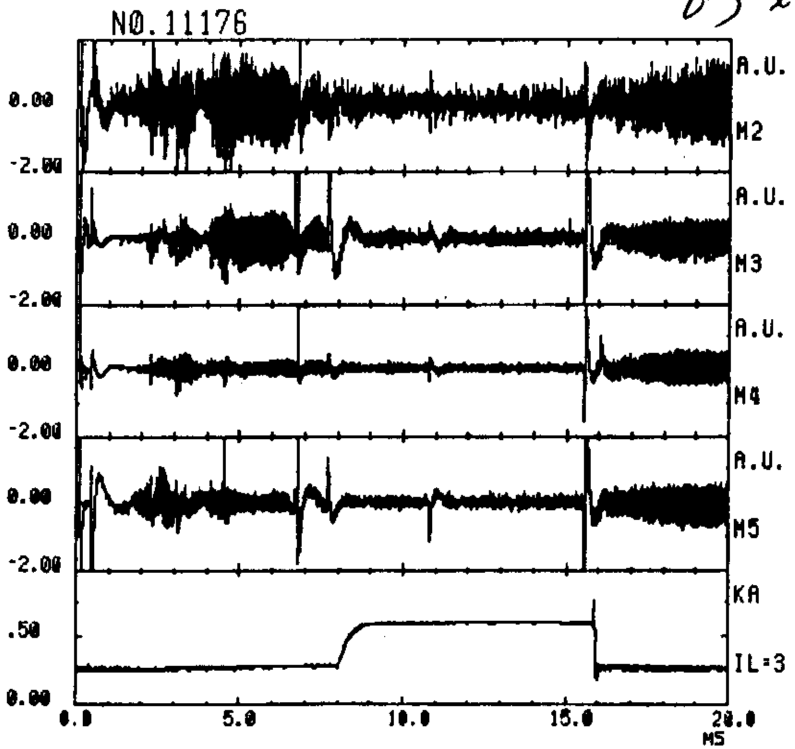

FIG.5B. GLOBLE MODE EFFECT OF RHF IL=3.

A1, A2

IBID.
860827D02.001

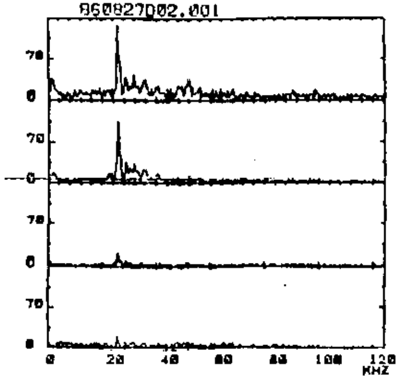

IBID. L=3. BEFORE·

INTERVAL 12.-14.9(MS) CH.21.22.23.2
860827D02.001

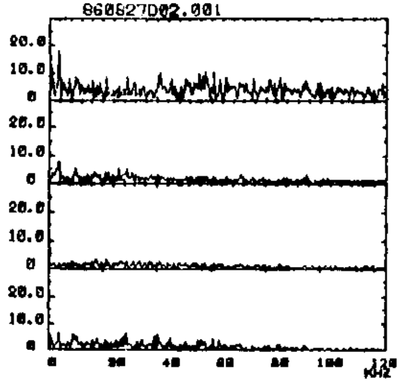

FFT SPECRA UNDER RHF L=3

INTERVAL 10.-20.(MS) 22.23.24.25.
860827D02.001

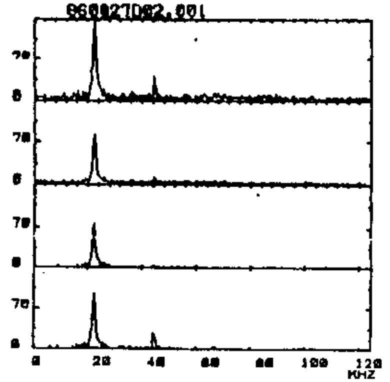

FFT SPECTRA AFTER RHF L=3

INTERVAL 12.-14.(MS) 22.23.24.25.
860901D06.001

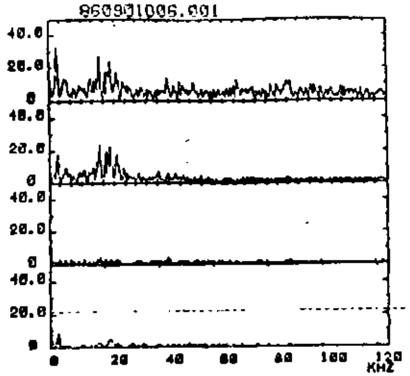

FFT SPECTRA UNDER RHF L=2·

INTERVAL 4.-6.(MS)22.23.24.25.
860901D06.001

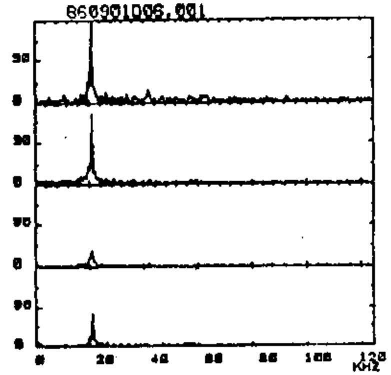

FFT BEFORE RHF L=2

INTERVAL 10.-20.(MS) M=2.3.4.5.
860901D06.001

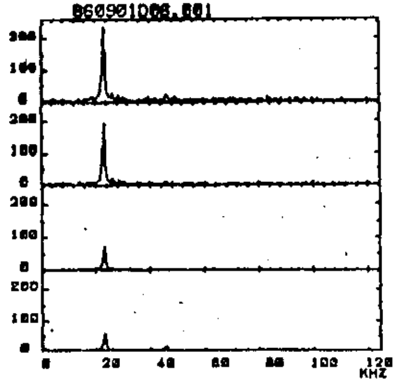

FFT SPECTRA AFTER RHF L=2

A3

5. Larger L=2 RHF(5% Of B_p) could destroy the plasma, but suitable L=3 RHF can protect the plasma from it. The larger L=2 field excit all other m components of magnetic fluctuation except m=3, which is suppressed by L=3 RHF.

850821D021.001

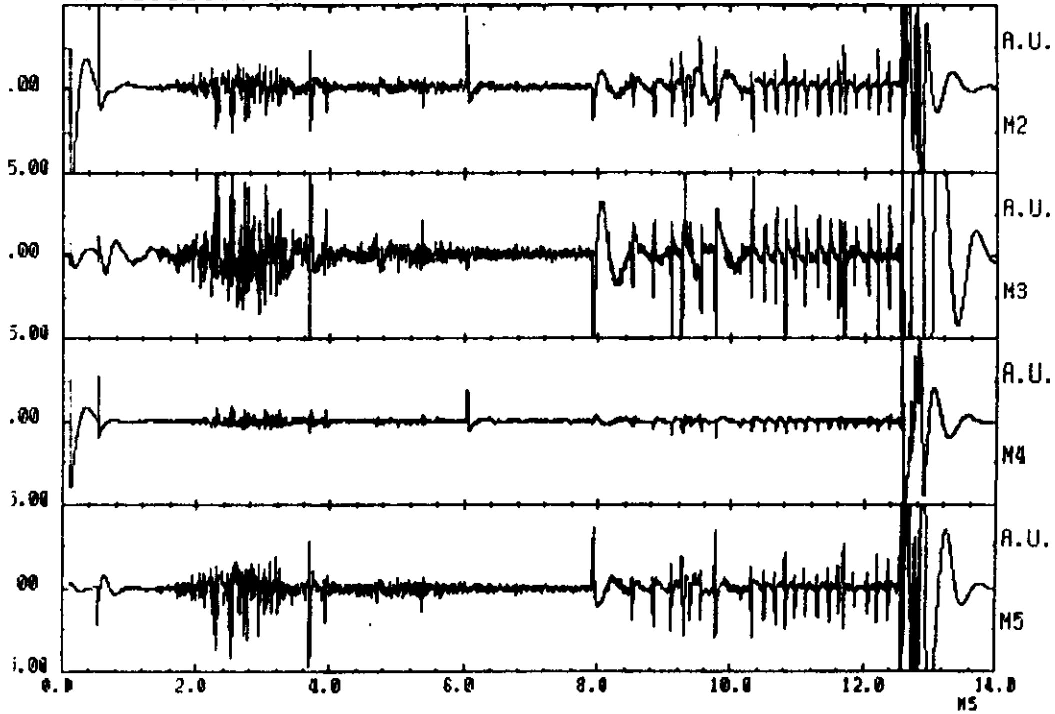

FIG.8. MUTUAL EFFECT BETWEEN IL=2 AND IL=3

Controll the disruption!

A4

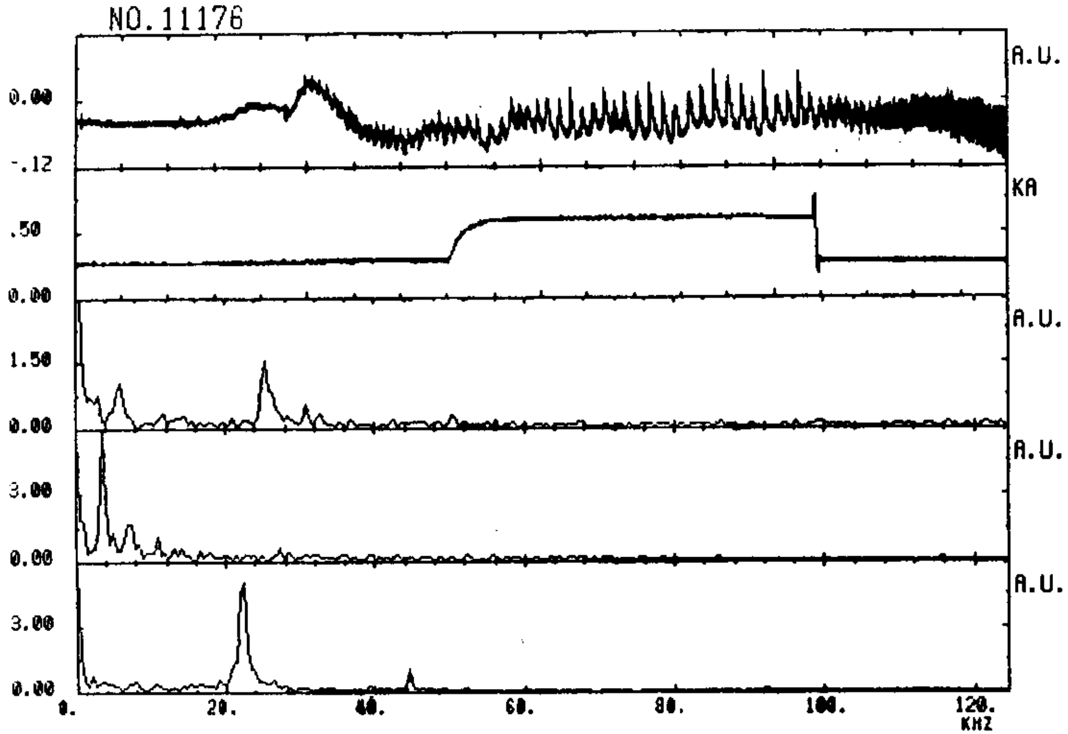

FIG.6B. INFLUENCE OF RHF L=3 ON SXF

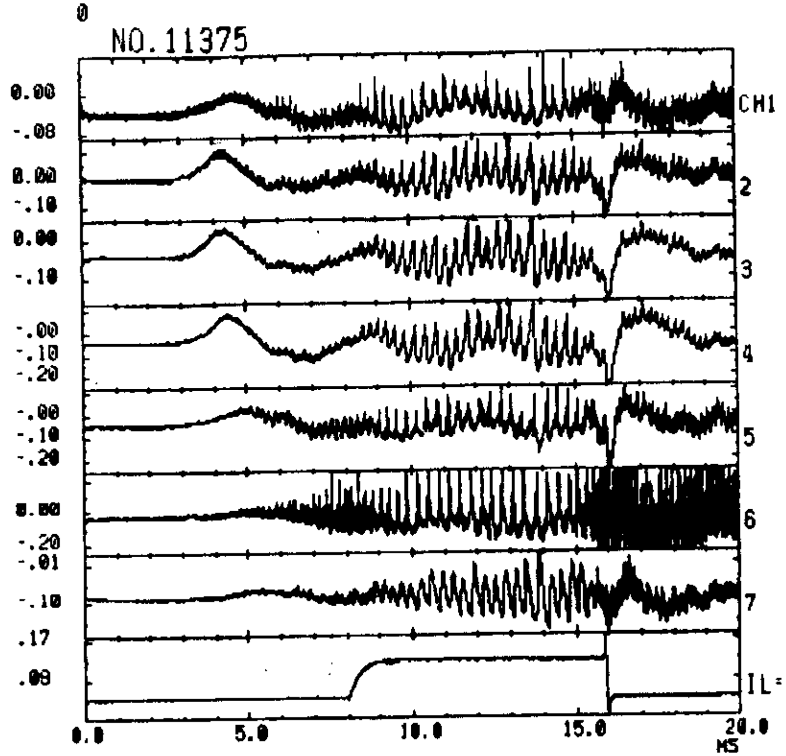

FIG. . EFFECT OF RHF ON TOTLE TYPE-2 SX

FIGURE CAPTIONS

Fig. 1.a T/T(0) vs r/a for six, low q_L ohmic discharges. Here q_L = 2.65, 2.65, 2.70, 2.79, 3.39, 3.41; $\int$ ndl = [illegible].8, 6.6, 4.0, 2.1, 2.0 × $10^{19} m^{-2}$; B = 4.66, 4.66, 4.80, 4.76, 5.81, 3.05 T; R = 2.59, 2.59, 2.56, 2.57, 2.07, 2.79 m; a = 0.80, 0.80, 0.82, 0.82, 0.41, 0.58 m; respectively.

1.b T/T(0) vs r/a for four, low q_L, neutral beam heated discharges. Here q_L = 2.65, 2.65, 2.67, 2.65; $\int$ ndl = 6.9, 8.7, 9.[illegible], 9.3 × $10^{19} m^{-2}$; B = 4.66, 4.66, 4.83, 4.79 T; R = 2.59, 2.59, 2.49, 2.49 m; a = 0.8, 0.80, 0.83, 0.83 m; the injected power P_B = 4.20, 4.26, 10.50, 9.56 MW; respectively.

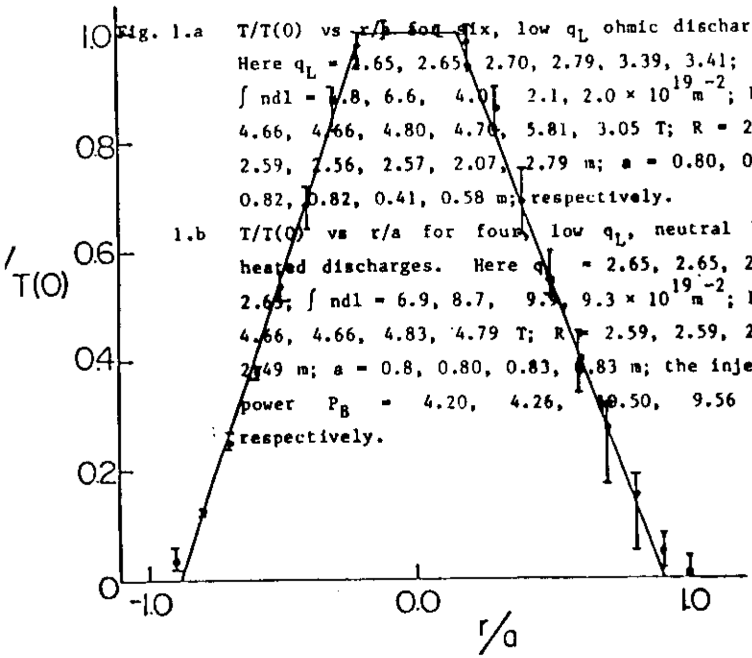

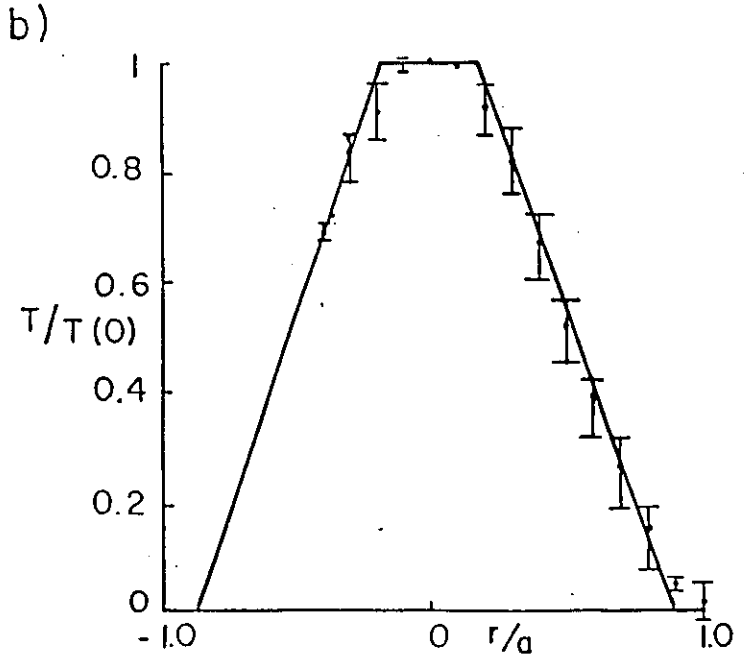

Fig. 1

A6

discharges. Here q_L = 7.47, 7.87, 7.88; $\int$ ndl = 1.0, 1.3, 1.4 × $10^{19} m^{-2}$; B = 3.90, 4.72, 4.72 T; R = 2.55, 2.56, 2.56 m; a = 0.82, 0.82, 0.82 m; respectively.

2.b T/T(0) vs r/a for six, mid-high q_L, neutral beam heated discharges. Here q_L = 7.91, 7.88, 4.70, 4.73, 4.72, 4.72; $\int$ ndl = 2.[illegible], 3.5, 4.8, 4.9, 4.[illegible], 4.9 × $10^{19} m^{-2}$; B = 4.72, 4.73, 4.8, 4.8, 4.7, 4.[illegible] T; R = 2.56, 2.55, 2.48, 2.48, 2.48, 2.48 m; a = 0.82, 0.82, 0.83, 0.83, 0.83, 0.83 m; P_B = 4.23, 4.91, 11.0, 10.49, 11.31, 10.42 MW; respectively.

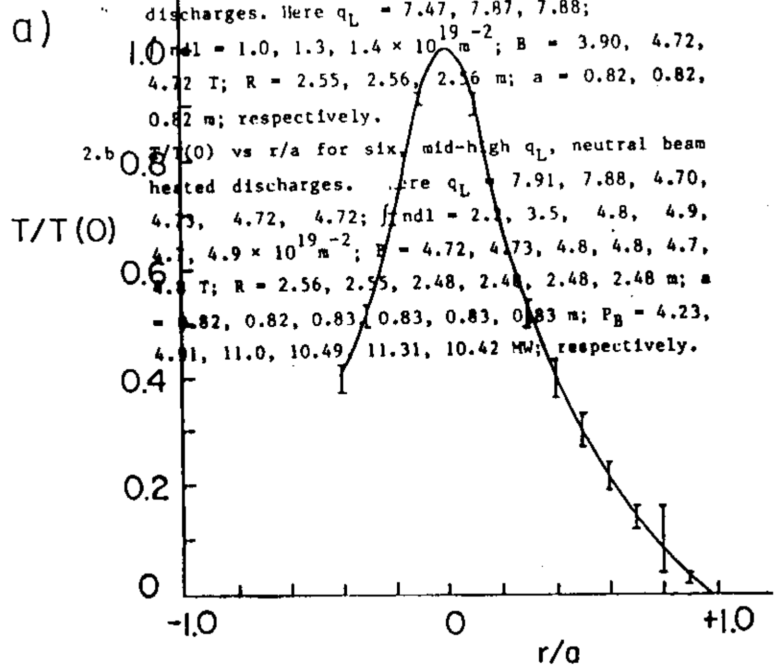

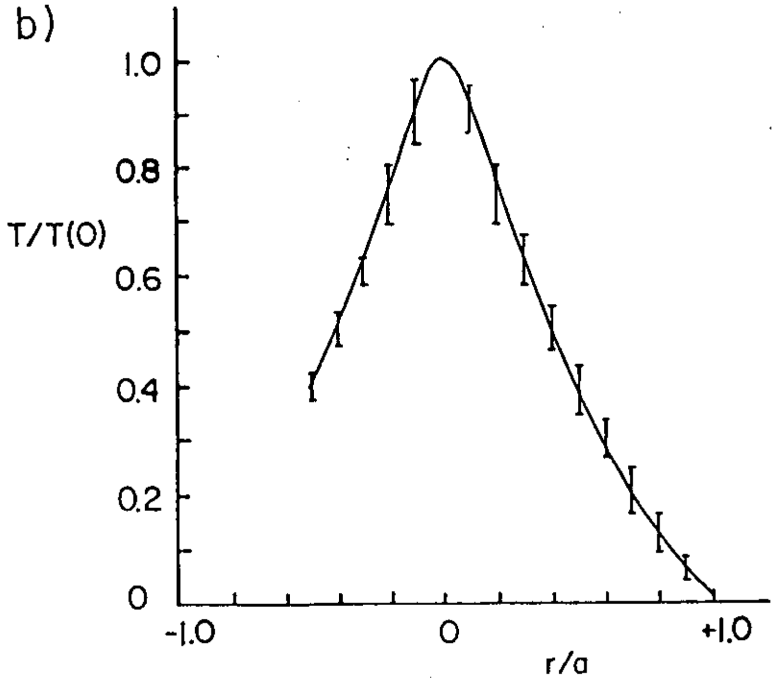

Fig. 2